# ORIGINAL ARTICLES

## Synthesis And Characterization Of Cordierite From Serpentinite, Kaolinitic Clay And Bauxite

**[1]Mazin Y. Tamar-Agha, [2]Ahmad M. Aqrawi and [1]Mohammad Essam S. Al-Hassan**

[1]*Department of Earth Sciences, College of Science, University of Baghdad, Jadiriya, Baghdad- Iraq.*
[2]*Department of Geology, College of Science, Salahaddin University, Erbil-Iraq.*

## ABSTRACT

Cordierite ($2MgO.2Al_2O_3.5SiO_2$) was synthesized from beneficiated serpentinite, kaolinitic clay and/or bauxite. The raw materials were chemically analysed for their major constituents, then crushed and ground to less than 35 μm. The work incorporated two stages. In the first stage four mixes were prepared using proportions of the raw materials near to the stoichiometric composition of cordierite, and then cold pressed under 1000 kg/cm$^2$ using about 10% water. The hydraulic formed samples were oven-dried and fired at 1100, 1200 and 1300 $^o$C with a heating rate of 1 $^o$C /minute. In the second stage, four mixes were prepared by adding mineralizers to the mixes that yielded more cordierite in the first stage. The mineralizers were either 2 wt% of LiF or 1 wt% of LiF and 1 wt% of NaF. These mixes were thoroughly mixed and ground for one hour to obtain better homogeneity and initiate a mechanochemical reaction. Test discs were hydraulically formed, dried and fired by the same procedure as above. X-ray diffractometry of the fired test discs revealed that forsterite and corundum were present in the samples fired at 1100 $^o$C. Cordierite first appeared in the samples fired at 1200 $^o$C in association with forsterite or mullite, according to the available excess oxides in the mixes. The addition of mineralizers led to the formation of cordierite at lower temperature (1100 $^o$C) in two forms namely α- and μ-cordierites, which were both, converted to indialite (stable form) at higher temperatures. The thermal properties of the studied test discs showed an inverse relationship between cordierite content and thermal conductivity and thermal expansion coefficient. On the other hand there is a direct relationship with thermal shock resistance.

*Key words:* cordierite, serpentinite, kaolin, bauxite, thermal insulators and electrical insulators

## Introduction

Cordierite is used in industrial ceramics and refractories especially for its high thermal shock resistance and low thermal expansion coefficient. Grosjean summarized its uses in refractory products, such as kiln furniture, sagger, gas burners and flame guards, in electro-ceramics as resistors and fuses and in flameproof tableware (Grosjean, P., 1993). Cordierite is also used in glazing of tiles as it improves its mechanical and chemical properties such as enhancing its resistance to abrasion and acids (Ferrari, A.M., *et al*., 1997). Recently some attempts were introduced to use cordierite for pollution control (Yamuna, A., *et al*., 2004).

It can be prepared by several methods such as the solid-state reaction and the sol-gel method (Grosjean, P., 1993; Naga, S.H., *et al*., 1994; Nakahara, M., *et al*., 1998; Trumbulović, Lj., *et al*., 2003; Khabas, T.A., *et al*., and Ghitulica, C., *et al*., 2007). In the solid-state reaction method several starting materials can be used such as single, double and triple compounds. Single compounds include oxides, carbonates or hydroxides of Mg, Si and Al, double compounds such as kaolin and talc, and triple compounds such as chlorite, which incorporates all constituting oxides. Double and triple compounds are favored, especially in hydrated forms, because the major constituents would be present with hydroxyl bonding and during heating they liberate the constitutional water, which in turn facilitate the reaction and gives wider sintering range (Grosjean, P., 1993; Trumbulović, Lj., *et al*., 2003; Khabas, T.A., *et al*., and Ghitulica, C., *et al*., 2007). The sol-gel method incorporates metallic salts for instance magnesium acetates, silicon elchoxide and aluminus-butoxide (Barrier, J.C., *et al*., 1986). These compounds are good for lowering the reaction temperature but they are rather expensive compounds (Nakahara, M., *et al*., 1999).

Cordierite is characterized by narrow sintering range, about 25 – 30 $^o$C, at its melting temperature (1455 $^o$C) and the rate of sintering is very sensitive to the impurity present (Morell, R., 1979). The firing range can be increased by the addition of Na-feldspar (Kingery, W.D., *et al*., 1976). Some oxides (such as titanium and bismuth oxides) and other chemical compounds (such as $AlF_3$, NaF and LiF) can be used as mineralizers, which cause nucleation and activate cordierite crystallization (Naga, S.H., *et al*., 1994; Morell, R., 1979 and Dupon, R.W., *et al*., 1990).

---

**Corresponding Author:** Mazin Y. Tamar-Agha, Department of Earth Sciences, College of Science, University of Baghdad, Jadiriya, Baghdad- Iraq.
E-mail: mtamaragha@yahoo.com

4947

*J. Appl. Sci. Res., 9(8): 4946-4959, 2013*

The aim of this work is to prepare cordierite from cheap, double or triple compounds (serpentinite, kaolinitic clay and/or bauxite) by solid-state reaction method. Moreover it is intended to characterize the product by investigating its sintering, mechanical, thermal and electrical properties.

**Materials And Methods**

Serpentinites crop out in many localities in the Thrust Zone, northeastern Iraq (Fig. 1), as part of Walash volcanosedimentary sequence (Palaeocene – Eocene). They are formed by hydrothermal metamorphism of ultrabasic igneous rocks. The serpentinite sample used here is brought from Galala Quarry – Erbil Governorate (Fig.1). It is currently quarried and used as dimension stones, crushed stones and in dolomite refractory products. Preliminary investigations showed that they contain impurities such as calcite and magnetite (Aqrawi, A.M.A., 2001). The kaolinitic clay used in this investigation represents overbank deposits of ancient fluvial system (Ga'ara Formation-Permocarboniferous) brought from Duekhla Mine, the western desert of Iraq. The bauxite is brought from the Hussainiyat Bauxite Mine (Jurassic) from paleokarsts, the western desert of Iraq too.
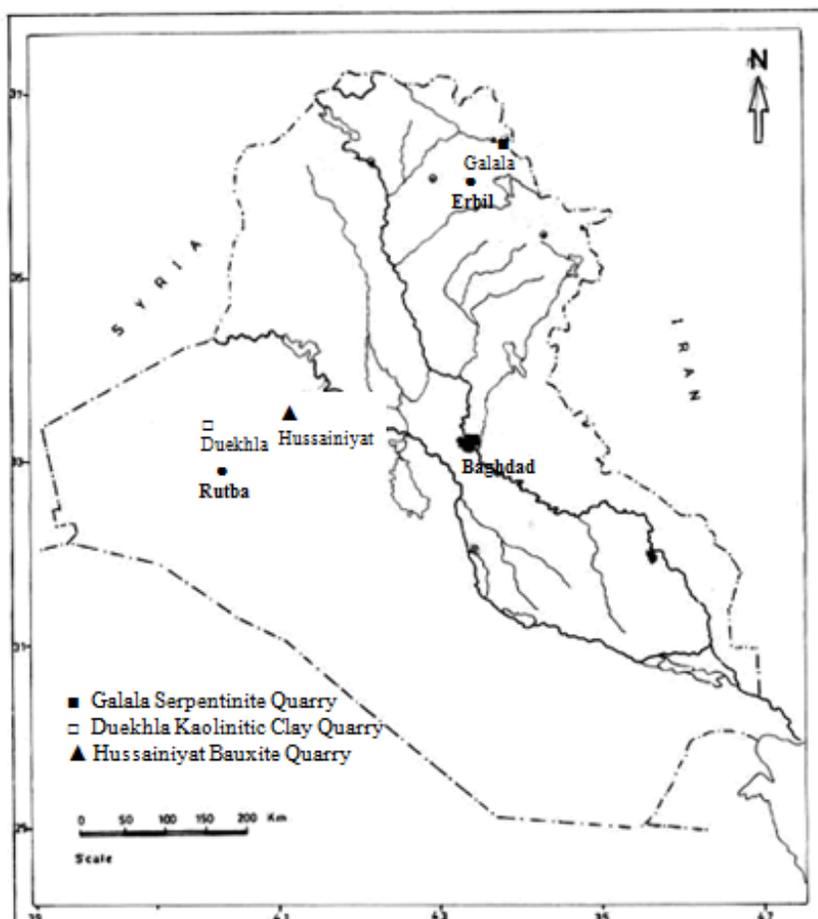


**Fig. 1:** Sample locations of the raw materials.

The raw materials were crushed, ground to grain size less than 35 μm, thoroughly mixed and chemically analyzed for their major constituents. All major constituents except loss on ignition (L.O.I) were analyzed by atomic absorption spectrophotometry (AAS) in the laboratories of the Iraqi State Company of the Geological Survey and Mining - Baghdad. The mineralogy was carried out using a monochromtized Cu Kα X-ray diffractometer (Model PW 1130, Philips) at the Department of Geology – University of Baghdad. DTA was carried out using a thermal analyser (Model STA-409, NETZSCH) and thermogravimetry using Stanton Redcroft TG76-Series at the Building Research Council - Baghdad.

The serpentinite was treated with weak HCl (10%) to remove impurities such as calcite, and then washed, dispersed with sodium hexametaphosphate and the magnetite was separated with hand magnet. Two stages of work were executed; in the first stage four mixes (A, B, C and D) were prepared using proportions of the raw materials near to the stoichiometric composition of cordierite (Table 1). Each mix is thoroughly mixed in a

4948

*J. Appl. Sci. Res., 9(8): 4946-4959, 2013*

porcelain ball mill for 2 hours in order to reduce particle size further and to attain complete homogeneity. Disc samples were formed by semi-dry pressing in a stainless steel mould (3 cm diameter) under 1000 kg/cm$^2$ using about 10% water. The hydraulic formed samples were oven-dried for 24 hours at 110 $^o$C and fired at 1100, 1200 and 1300 $^o$C with a heating rate of 1 $^o$C /minute and one hour soaking time. In the second stage, another four mixes were prepared by adding mineralizers to the mixes that yielded more cordierite in the first stage that is mixes C and D. The mineralizers were either 2 wt% of LiF or 1 wt% of LiF and 1 wt% of NaF. These mixes were thoroughly mixed and ground for one hour to obtain better homogeneity and initiate a mechanochemical reaction. Test discs were hydraulically formed, dried and fired following the same procedure as above. The highest firing temperature considered in this work is 1300 $^o$C because some workers considered 1250 $^o$C as safe operating temperature (Kingery, W.D., *et al.*, 1976 and Singer, F. and S. Singer, 1971) and others suggested 1280 to 1300 $^o$C as the most suitable temperature for cordierite crystallization (10 and 16).

Apparent porosity, water absorption and bulk density of the fired test discs were measured following ASTM C373-72. Volumetric shrinkage and thermal shock resistance were measured as in Chester (1973). Thermal conductivity was measured in room temperature by Lee's method whereas a heating microscope measured modulus of thermal expansion.

**Table 1:** Percentages of the raw materials used in the mixes.

| Mix | Serpentinite | Kaolinitic Clay | Bauxite | NaF | LiF |
|-----|--------------|-----------------|---------|-----|-----|
| A | 50 | 50 | - | - | - |
| B | 30 | 60 | 10 | - | - |
| C | 28 | 57 | 15 | - | - |
| D | 27 | 64 | 9 | - | - |
| C$_1$ | 28 | 57 | 15 | - | 2 |
| D$_1$ | 27 | 64 | 9 | - | 2 |
| C$_2$ | 28 | 57 | 15 | 1 | 1 |
| D$_2$ | 27 | 64 | 9 | 1 | 1 |

## Results And Discussions

*Raw Materials:*

X-ray diffractograms reveal that the serpentinite consists mostly of chrysotile as clinochrysotile and orthochrysotile with subordinate magnetite and calcite (Fig. 2a). DTA curve of the serpentinite shows two endothermic peaks (Fig. 3a): the first at 665 $^o$C representing the dehydration of the serpentine minerals whereas the second peak at 785 $^o$C representing the decomposition of the mineral structure (Kloss, W. S., 1974). One exothermic peak is found at 835 $^o$C that representing the crystallization of forsterite. TG and DTG thermograms (Fig. 4a) show that it looses its hygroscopic water at 124 $^o$C and starts losing its constitutional water at 663 $^o$C (Kloss, W. S., 1974). At 805 $^o$C it looses all its constitutional water, which makes about 11.6% of its weight. Chemical analyses of the beneficiated serpentinite showed that the constituents of the serpentine minerals (MgO, SiO$_2$ and L.O.I) totals to about 96% of the sample (Table 2) whereas total iron oxides are about 2%.

X-ray diffraction of Duekhla Clay shows that kaolinite is the predominant mineral (about 85%) with minor amount of quartz (about 10%) and traces of illite-smectite mixed-layer (Fig. 2b). DTA curve of the clay sample reveals the presence of two endothermic peaks (Fig. 3b) at 250 and 540 $^o$C and one exothermic peak at 950 $^o$C. The first endothermic peak is attributed to the dehydroxylation of the illite-smectite mixed-layer; the second endothermic peak is attributed to the dehydroxylation of the kaolinite whereas the exothermic peak is attributed to the formation of mullite and cristobalite. TG and DTG thermograms (Fig. 4c) show that it loses its non-constitutional water at 95-140 $^o$C and it dehydroxylate at 500-580 $^o$C. The total loss of weight is about 10.9%. The chemical analyses showed that SiO$_2$, Al$_2$O$_3$ and L.O.I make about 96% of the clay sample (Table 2).

The XRD pattern of bauxite sample reveals the presence of major minerals such as boehmite (about 60%) and kaolinite (about 38%) with minor amount of gibbsite (Fig. 2c). It is accordingly kaolinitic bauxite. DTA curve of the bauxite sample show two broad endotherms at 350 and 590 $^o$C (Fig. 3c), which represent dehydroxylation of boehmite-gibbsite and kaolinite respectively. Broadening of the peaks could be attributed to degree of crystallinity, disorder, particle size of the minerals and the overlap of the peaks. TG and DTG thermograms (Fig. 4b) show that it looses about 2.2% of its weight at 360 $^o$C due to gibbsite dehydroxylation and 13.1% of its weight at 650 $^o$C due to total loss of water in the sample. The chemical analyses of the bauxite show that its alumina content is about 65% and SiO$_2$, Al$_2$O$_3$ and L.O.I make about 96.5% of the sample.

K: Kaolinite
Q: Quartz
G: Gibbsite
Bo: Boehmite
A: Anatase
I/S: Illite-smectite
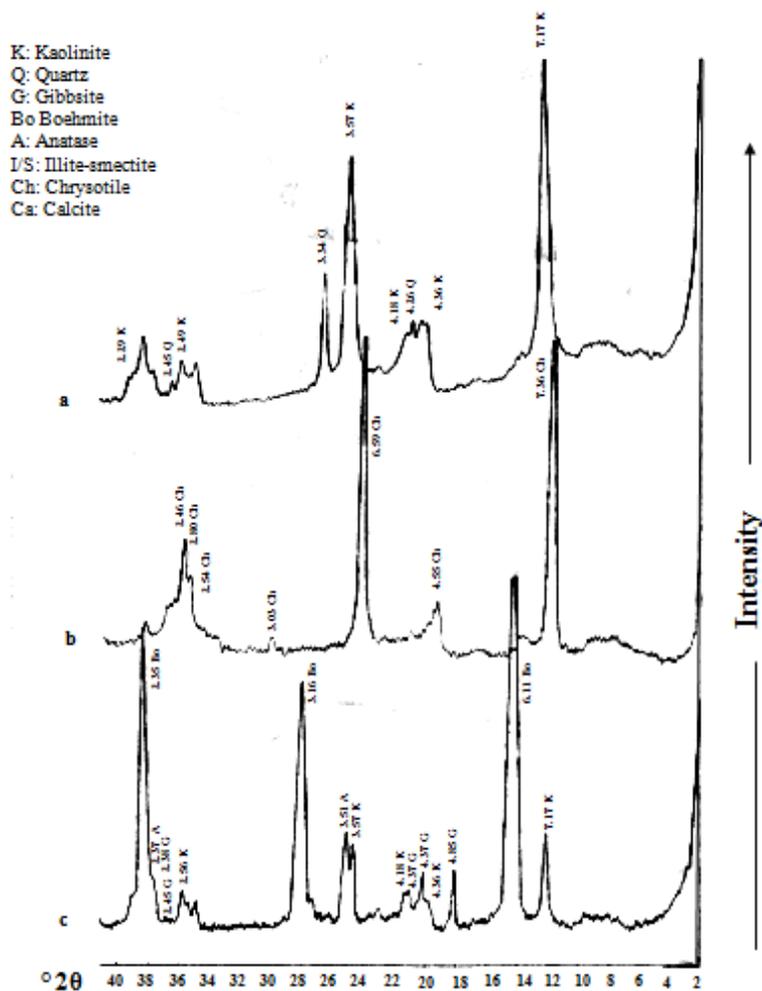Ch: Chrysotile
Ca: Calcite



**Fig. 2:** X-ray diffractograms of the raw materials used in the study: a- Duekhla Kaolinitic Clay, b- Serpentinites and c- Hussainiyat Bauxite.
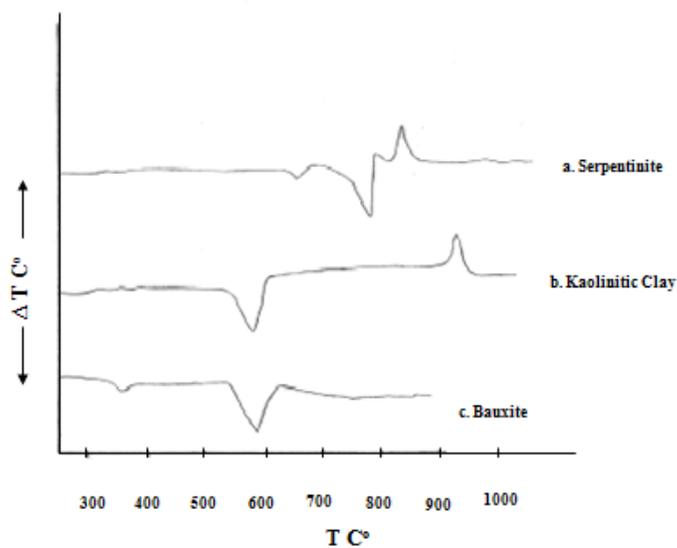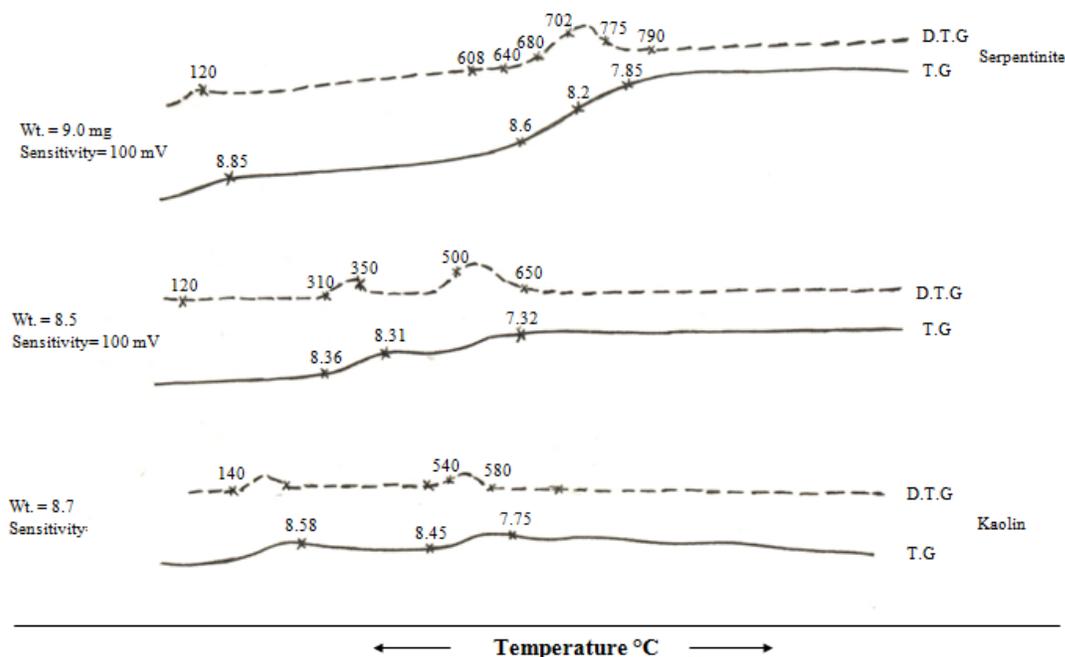


**Fig. 3:** DTA curves of the raw materials used in the study: a- Serpentinites, b- Duekhla Kaolinitic Clay and c- Hussainiyat Bauxite.

**Fig. 4:** TG and DTG of the raw materials used in the study: a- Serpentinites, b- Duekhla Kaolinitic Clay and c-Hussainiyat Bauxite.

**Table 2:** Chemical analyses of the raw materials used showing the major and minor constituents only.

| Raw Material | SiO₂ % | Al₂O₃ % | Fe₂O₃ % | TiO₂ % | MgO % | CaO % | L.O.I. % | Total % |
|---|---|---|---|---|---|---|---|---|
| Serpentinite | 41.16 | 1.48 | 2.18 | - | 43.49 | - | 11.60 | 99.91 |
| Kaolinitic Clay | 49.56 | 34.85 | 1.35 | 1.23 | 0.53 | 0.10 | 12.40 | 99.02 |
| Bauxite | 17.98 | 64.95 | 1.20 | 1.50 | - | 0.20 | 13.76 | 99.59 |

*Mineral Transformations:*

The XRD diffractograms of the fired samples reveal that the mineral transformations are function of the raw materials, mineralizers and firing temperature. The samples fired at 1100 °C are composed chiefly of quartz, clinoenstatite and forsterite as well as traces of mullite and corundum (Figs. 5, 6, 7 and 8). The samples fired at 1200 °C are composed of α-cordierite, mullite, forsterite and protoenstatite with traces of spinel whereas those fired at 1300 °C are composed mostly of cordierite with traces of forsterite, mullite, spinel, cristobalite and periclase. Such phase transformations complies with the previous literature (Morell, R., 1979 and Trumbulović, Lj., *et al*., 2003). The presence of these traces depends on the composition and proportion of starting materials or that the reaction is yet incomplete. In sample D, both spinel and periclase are formed as a result of the low content of alumina and silica in the mix. However in order to overcome such a problem a slight alteration is necessary either in the mix or in the firing program (that is either raising the firing temperature or lengthening the soaking time). Instead the addition of mineralizers has led to the crystallization of cordierite at lower temperatures, as α- and μ-cordierite are found in the samples fired at 1100 °C as well as quartz or cristobalite with traces of mullite, forsterite, protoenstatite and spinel (Figs. 9 and 10). The amount of α- or μ-cordierite formed depends on the mineralizer added. The addition of NaF+LiF to the mix leads to crystallization of more μ-cordierite than α-cordierite, whereas the addition of LiF alone, higher amount of α-cordierite is formed. Firing the samples at 1300 °C indialite is formed (a high variety of cordierite) with traces of spinel, mullite or protoenstatite (Fig. 10).
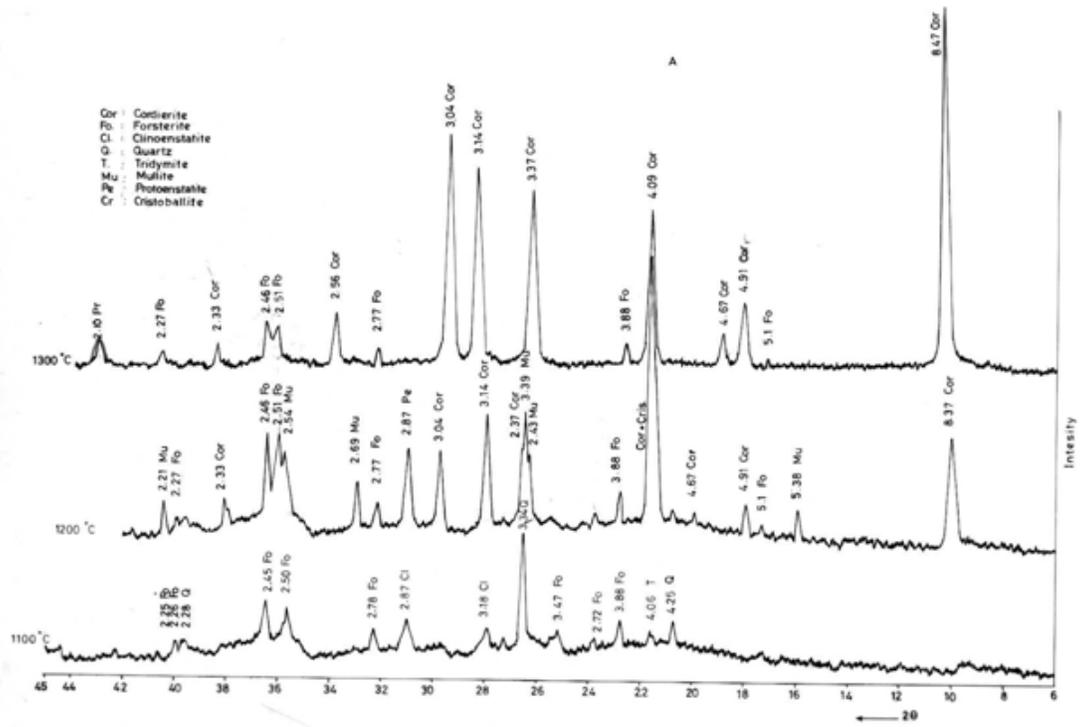
**Fig. 5:** X-ray diffractogram of test discs of mix A fired at 1100 °, 1200 ° and 1300 °C.

**Fig. 6:** X-ray diffractogram of test discs of mix B fired at 1100 °, 1200 ° and 1300 °C.

**Fig. 7:** X-ray diffractogram of test discs of mix C fired at 1100 °, 1200 ° and 1300 °C.
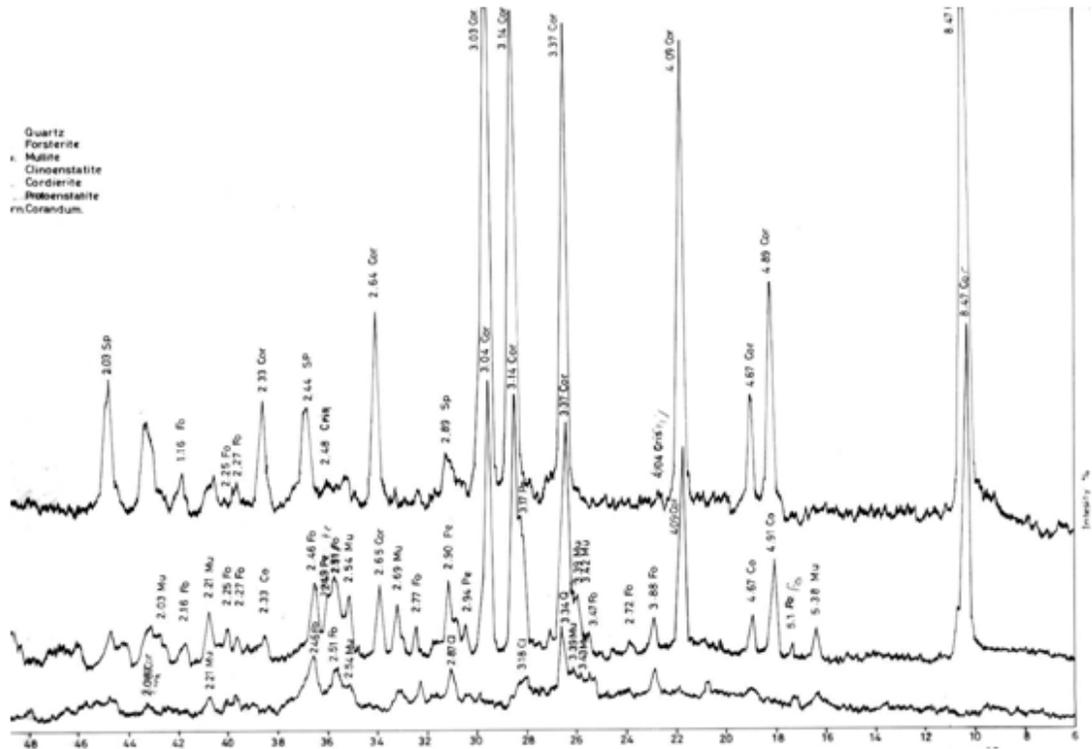


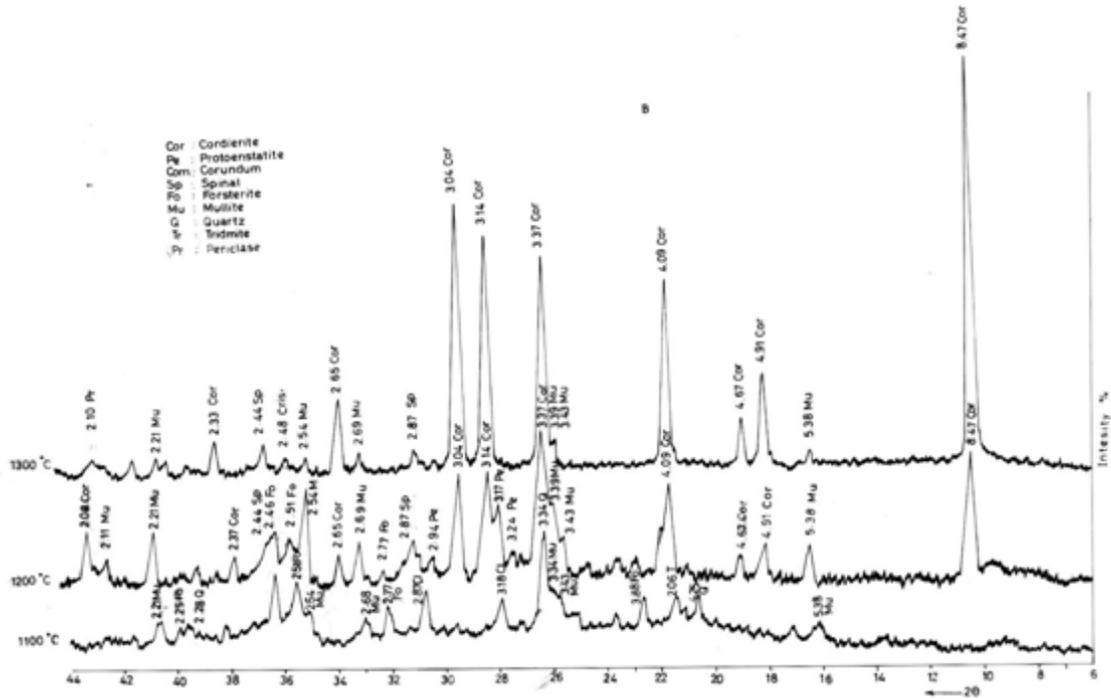**Fig. 8:** X-ray diffractogram of test discs of mix D fired at 1100 °, 1200 ° and 1300 °C.

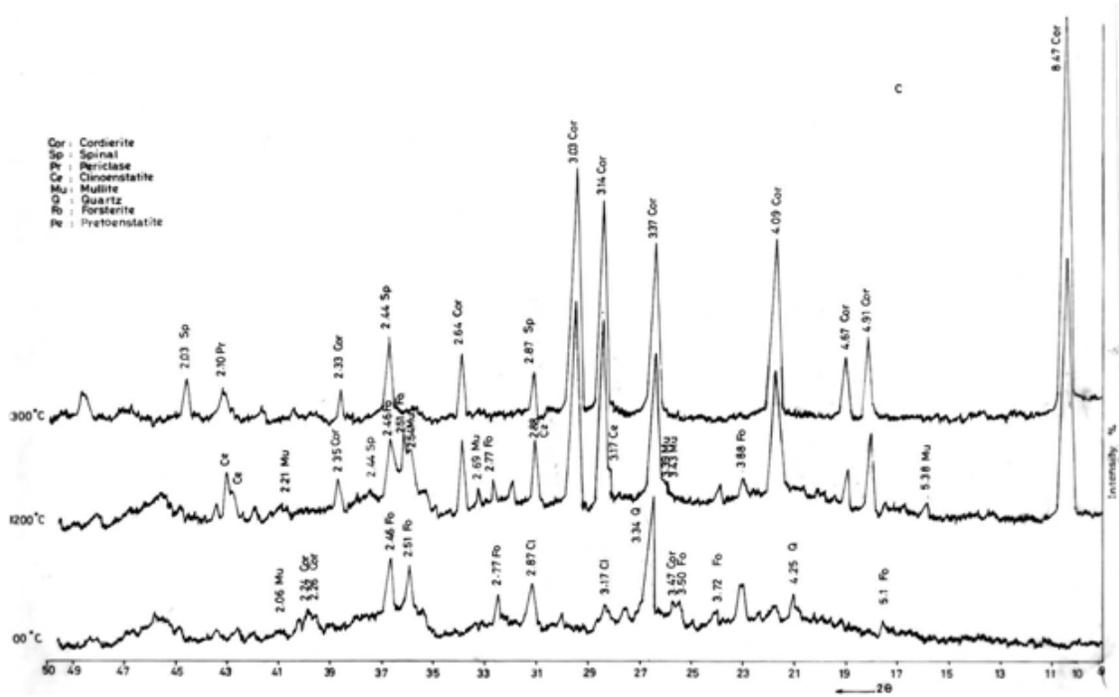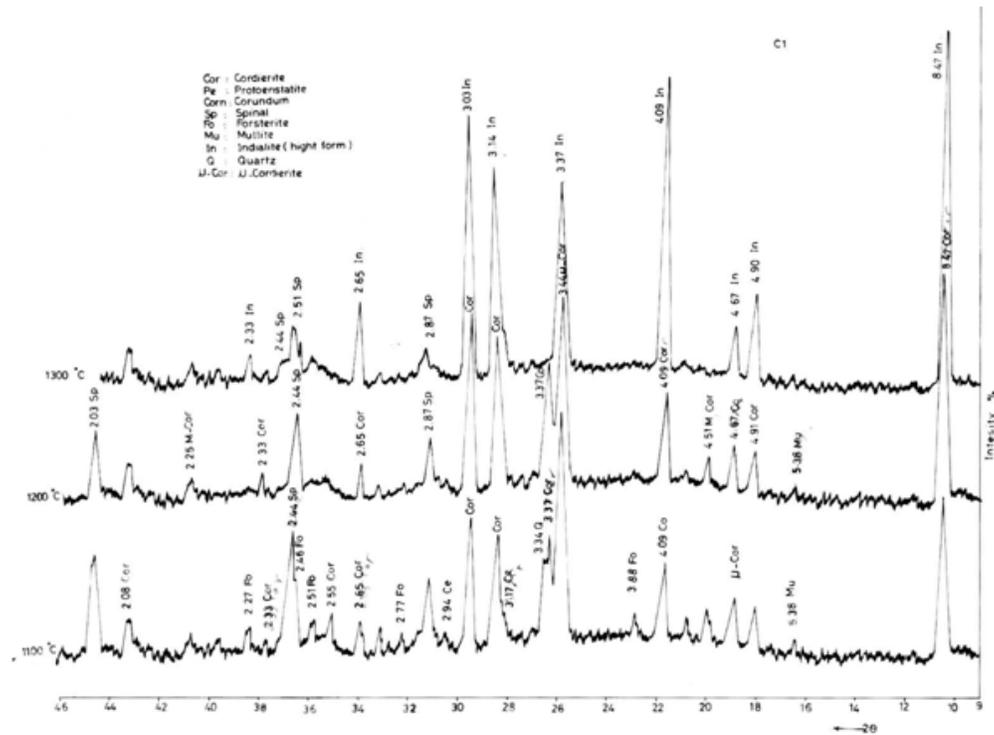**Fig. 9:** X-ray diffractogram of test discs of mix D1 fired at 1100 °, 1200 ° and 1300 °C.
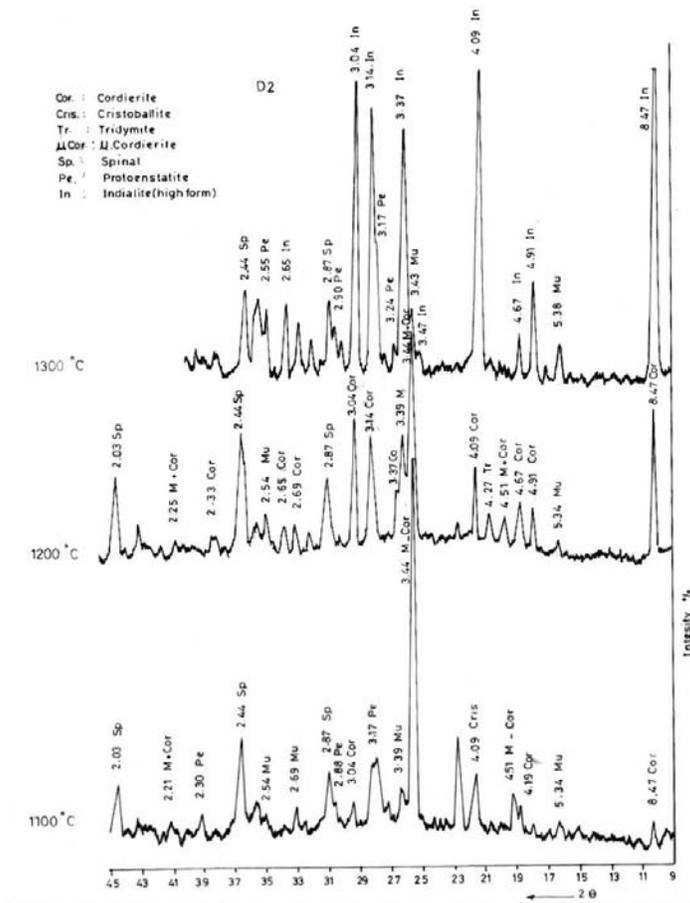


**Fig. 10:** X-ray diffractogram of test discs of mix D2 fired at 1100 °, 1200 ° and 1300 °C.

■ Apparent porosity                    ■ Bulk density
◆ Volume shrinkage                     ◆ Water absorption
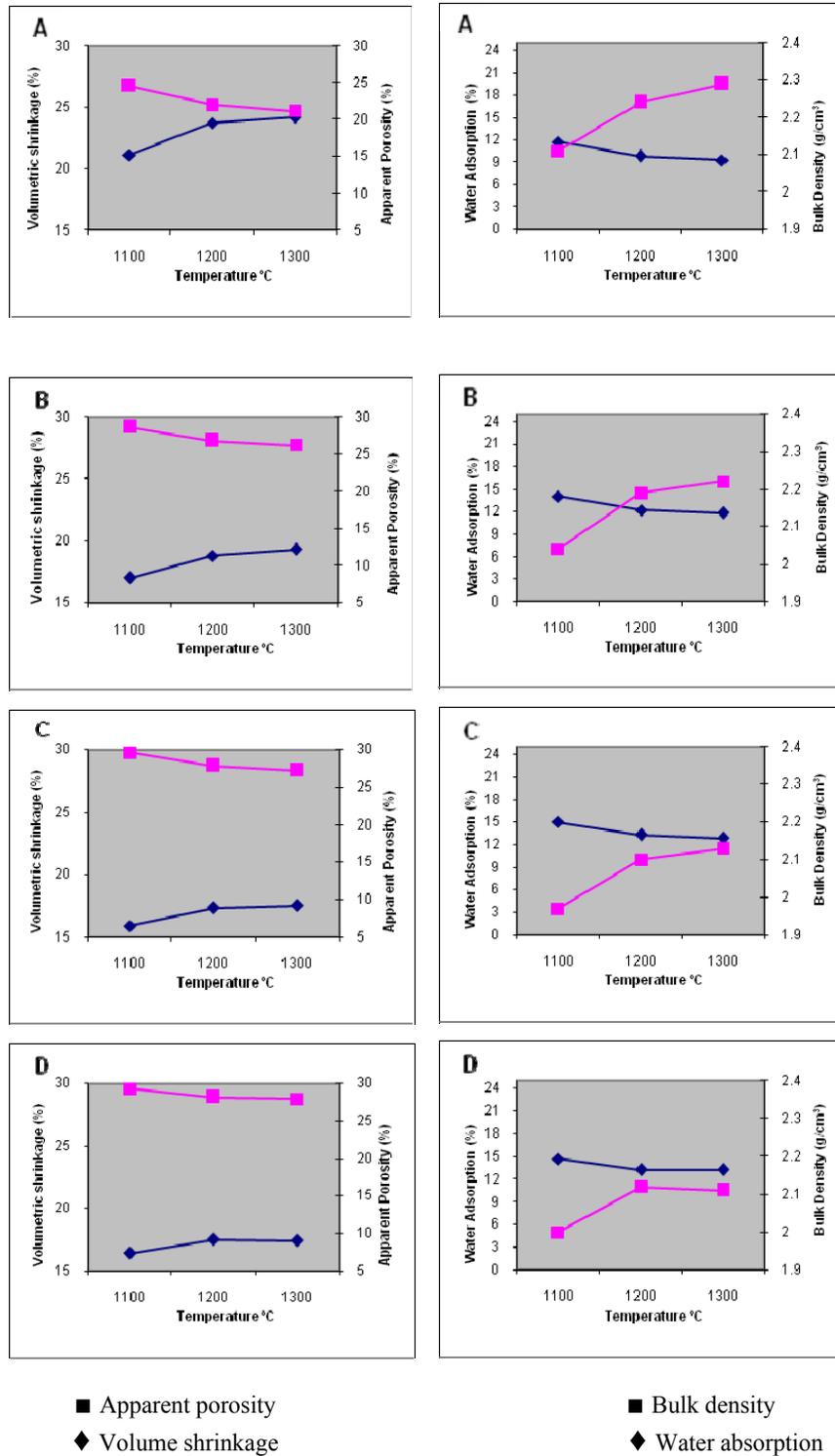
**Fig. 11:** The relationship between sintering properties vs. firing temperature for test discs A, B, C, and D.

*Sintering Properties:*

The physical tests show that the volume shrinkage and the bulk density have direct relationship with firing temperature (Figs. 11 and 12, and Table 3). The increase of volume shrinkage and bulk density is noticeably

higher at 1200 $^{o}$C than at 1100 $^{o}$C whereas at 1300 $^{o}$C the increase is rather insignificant. The increase in volume shrinkage and bulk density is attributed to both mineral phase transformations and sintering. The mineral phases formed at firing temperature 1200 $^{o}$C are denser than those formed at 1100 $^{o}$C and at 1300 $^{o}$C almost only cordierite is formed. The former set of mineral phases is denser than the latter set. Nakahara and co-workers (Nakahara, M., *et al*., 1998) attributed the high shrinkage and bulk density to the formation of relatively higher density minerals phases.



**Fig. 12:** The relationship between sintering properties vs. firing temperature for test discs C$_1$, C$_2$, D$_1$ and D$_2$.
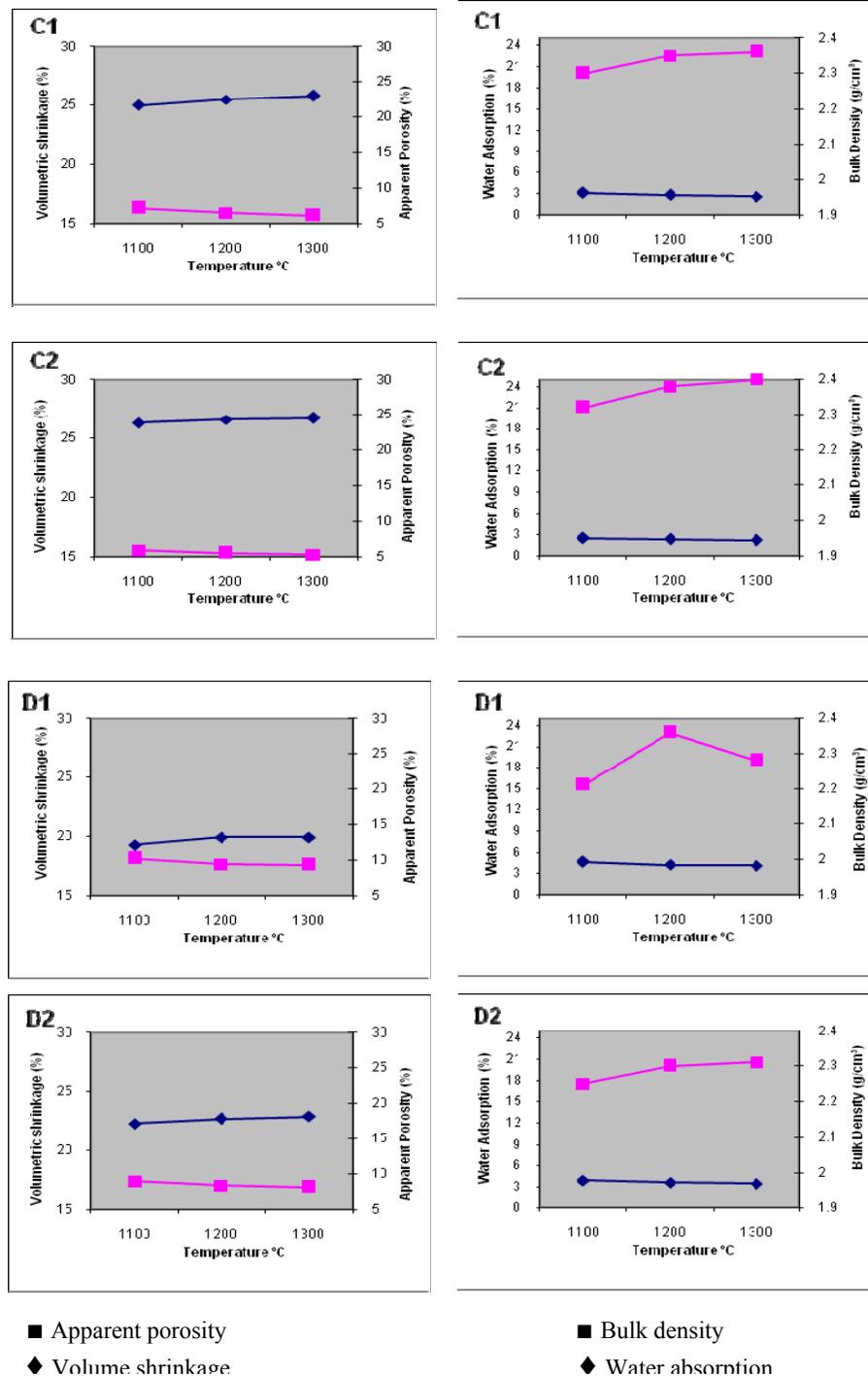
4956

*J. Appl. Sci. Res., 9(8): 4946-4959, 2013*

The apparent porosity and water absorption have inverse relationship with the firing temperature (Figs 11 and 12). The high porosity at 1100 $^o$C can be attributed to the high free silica content (El-Arabaty, A., *et al*., 1975) as well as to a lesser degree of sintering. The sharp decrease in the porosity and water absorption at 1200 $^o$C can be attributed to the crystallization of clinoenstatite, mullite, forsterite and spinel whereas the increase of porosity and water absorption at 1300 $^o$C is due to the crystallization of cordierite. SEM observations show the presence of both open and closed porosity and the latter is found in the intraparticle (Fig. 13).

**Table 3:** Sintering properties of the test discs fired at temperatures 1100°C, 1200°C and 1300°C.

| Mix | Firing temperature (°C) | | | | | | | | | | | |
| | 1100 | | | | 1200 | | | | 1300 | | | |
| | V.S % | A.P % | W.A % | B.D % | V.S % | A.P % | W.A % | B.D % | V.S % | A.P % | W.A % | B.D % |
|---|---|---|---|---|---|---|---|---|---|---|---|---|
| A | 21.1 | 24.6 | 11.7 | 2.11 | 23.7 | 22.0 | 9.8 | 2.24 | 24.2 | 21.2 | 9.3 | 2.29 |
| B | 17.0 | 28.6 | 14.0 | 2.04 | 18.8 | 26.8 | 12.2 | 2.19 | 19.3 | 26.2 | 11.2 | 2.22 |
| C | 15.9 | 29.6 | 15.0 | 1.97 | 17.3 | 27.8 | 13.3 | 2.10 | 17.5 | 27.2 | 12.8 | 2.13 |
| D | 16.4 | 29.3 | 14.7 | 2.00 | 17.5 | 28.1 | 13.2 | 2.12 | 17.4 | 27.9 | 13.2 | 2.11 |
| $C_1$ | 25.0 | 7.2 | 3.1 | 2.30 | 25.5 | 6.5 | 2.8 | 2.35 | 25.8 | 6.1 | 2.6 | 2.36 |
| $C_2$ | 26.3 | 5.9 | 2.5 | 2.32 | 26.6 | 5.5 | 2.3 | 2.38 | 26.7 | 5.3 | 2.2 | 2.40 |
| $D_1$ | 19.3 | 10.2 | 4.6 | 2.21 | 19.9 | 9.4 | 4.2 | 2.36 | 19.9 | 9.3 | 4.1 | 2.28 |
| $D_2$ | 22.3 | 8.9 | 3.95 | 2.25 | 22.7 | 8.3 | 3.6 | 2.30 | 22.9 | 8.1 | 3.5 | 2.31 |

V.S: Volume shrinkage.
A.P: Apparent porosity.
W.A: Water absorption.
B.D: Bulk density.
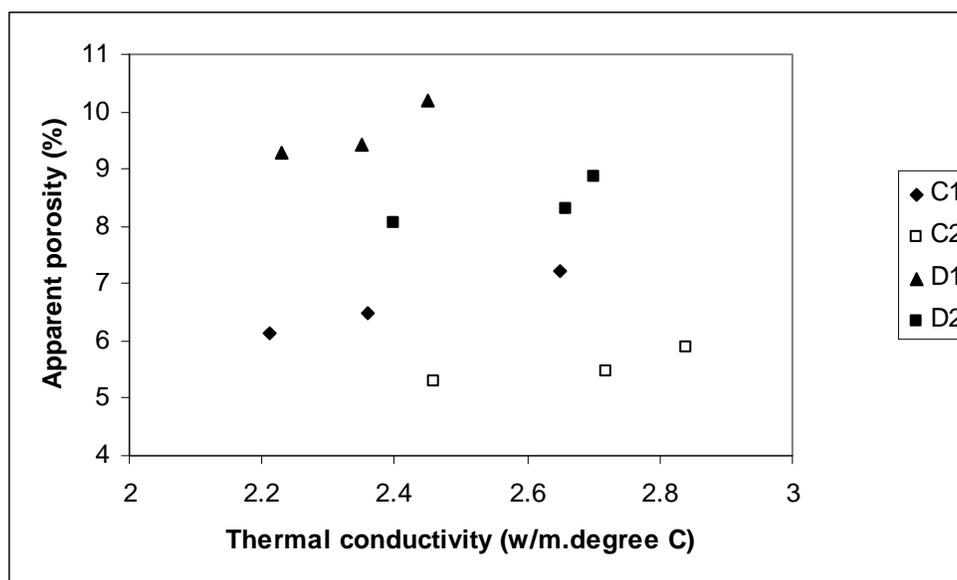


**Fig. 14:** Thermal conductivity of cordierite-rich test discs versus their porosity.

*Thermal Properties:*

The thermal conductivity of the test discs is dependent on their firing temperature (Table 4) and mineral composition as it shows a direct relationship with firing temperature and inverse relationship with cordierite content. It is evident that lesser serpentinite in the mix leads to crystallization of lesser forsterite and more silica in the test discs and in turn shows lower thermal conductivity. Lower values of thermal conductivity could be attributed to the higher content of silica at lower firing temperature, which has low thermal conductivity (1.44 W/m.$^o$C). At higher temperature other phases with higher thermal conductivity appear, such as spinel, clinoenstatite and mullite. Moreover, with higher firing temperature the porosity also decreases, which is another factor effective in raising thermal conductivity. Nevertheless, firing the test discs at higher temperature (1300 $^o$C) led to the crystallization of high amount of cordierite; this in turn led to dropping of the thermal conductivity. The addition of mineralizer to the mixes leads to the crystallization of cordierite at lower temperatures and in higher proportions. Accordingly thermal conductivity of the fired test discs shows different behavior; it drops with raising the firing temperature (Table 4) because the amount of cordierite increases. The effect of porosity on thermal conductivity is little (Fig. 14) in comparison to the percentage of formed cordierite

4957

*J. Appl. Sci. Res., 9(8): 4946-4959, 2013*

(Table 4). The addition of LiF alone to the mixes results in test discs with lower thermal conductivity in comparison with those that have both LiF and NaF to the mixes.

Thermal shock resistance is improved considerably by raising the firing temperature or by the addition of mineralizers (Table 4). There is a direct relationship between the thermal shock resistance of the fired test discs and their cordierite content. Samples, which consist almost entirely of cordierite, show high thermal shock resistance (30 cycles or more).

Coefficient of thermal expansion of the test discs fired at 1200 $^o$C ranged from 9.85 to 15.67 x $10^{-6}$/$^o$C (Table 5) whereas those fired at 1300 $^o$C ranged from 8.85 to 12.87 x $10^{-6}$/$^o$C. The difference in the value of thermal expansion is almost solely attributed to the phase present in the test discs. Sample A, for instance, when fired at 1200 $^o$C has higher coefficient of thermal expansion, as it contains higher content of protoenstatite and cristobalite, whereas it has lower coefficient of thermal expansion when fired at 1300 $^o$C as it contains higher cordierite. Sample $C_1$ has the lowest coefficient of thermal expansion as it contains the highest amount of cordierite in the samples of this study.

Small bowls (10x8 cm) were formed by plastic pressing of mixes A, B, C and D and fired at 1300 $^o$C. They survived through 15 cycles of heating (to red) and sudden cooling (by dropping in water), and this means that they are suitable for flameproof tableware.

**Table 4:** Thermal conductivity and thermal shock resistance of the test discs fired at temperatures 1100°C, 1200°C and 1300°C.

| Mix | Firing temperature (°C) | | | | | |
| | 1100 | | 1200 | | 1300 | |
| | T.C (w/m.°C) | T.S.R (no. of cycles) | T.C (w/m.°C) | T.S.R (no. of cycles | T.C (w/m.°C) | T.S.R (no. of cycles |
|---|---|---|---|---|---|---|
| A | 2.17 | 10 | 2.85 | 18 | 2.55 | 25 |
| B | 2.08 | 14 | 2.58 | 22 | 2.23 | 28 |
| C | 1.95 | 16 | 2.48 | 23 | 2.19 | >30 |
| D | 1.9 | 16 | 2.36 | 25 | 2.13 | 30 |
| $C_1$ | 2.65 | 20 | 2.36 | 24 | 2.21 | 30 |
| $C_2$ | 2.84 | 17 | 2.72 | 21 | 2.46 | 26 |
| $D_1$ | 2.45 | 22 | 2.35 | 28 | 2.23 | >30 |
| $D_2$ | 2.7 | 18 | 2.66 | 25 | 2.40 | 28 |

T.C: Thermal conductivity.
T.S.R: Thermal shock resistance.

**Table 5:** Thermal expansion (TE) and thermal expansion coefficient (TEC) of the test discs fired at temperatures 1100°C, 1200°C and 1300°C.

| Mix | A | | | | B | | | | C | | | | D | | | | $C_1$ | | | |
| | Firing Temperature °C | | | | | | | | | | | | | | | | | | | |
| Temperature °C | 1200 | | 1300 | | 1200 | | 1300 | | 1200 | | 1300 | | 1200 | | 1300 | | 1200 | | 1300 | |
| | T.E.C x$10^{-6}$ | T.E % | T.E.C x$10^{-6}$ | T.E % | T.E.C x$10^{-6}$ | T.E % | T.E.C x$10^{-6}$ | T.E % | T.E.C x$10^{-6}$ | T.E % | T.E.C x$10^{-6}$ | T.E % | T.E.C x$10^{-6}$ | T.E % | T.E.C x$10^{-6}$ | T.E % | T.E.C x$10^{-6}$ | T.E % | T.E.C x$10^{-6}$ | T.E % |
|---|---|---|---|---|---|---|---|---|---|---|---|---|---|---|---|---|---|---|---|---|
| 20-500 | 14.2 | 0.68 | 10.4 | 0.5 | 11.1 | 0.5 | 9.0 | 0.43 | 9.70 | 0.46 | 7.6 | 0.36 | 9.00 | 0.43 | 6.20 | 0.3 | 8.3 | 0.4 | 6.5 | |
| 20-750 | 15.5 | 1.13 | 11.6 | 0.85 | 12.7 | 0.93 | 10.7 | 0.78 | 10.50 | 0.76 | 9.10 | 0.66 | 10.2 | 0.75 | 9.50 | 0.7 | 9.5 | 0.7 | 8.9 | |
| 20-1000 | 16.1 | 1.58 | 12.2 | 1.2 | 13.6 | 1.30 | 11.2 | 1.10 | 11.00 | 1.08 | 9.80 | 0.96 | 11.3 | 1.12 | 10.3 | 1.02 | 10.5 | 1.03 | 9.6 | |
| 20-1200 | 16.0 | 2.00 | 13.8 | 1.63 | 14.1 | 1.50 | 12.7 | 1.50 | 12.10 | 1.43 | 11.10 | 1.32 | 12.7 | 1.50 | 11.7 | 1.04 | 11.1 | 1.32 | 10.5 | |
| Average | 15.67 | | 12.00 | | 12.88 | | 10.90 | | 10.83 | | 9.40 | | 10.80 | | 9.42 | | | | 8.87 | |

*Electrical Properties:*

Electrical properties of the fired test discs are assessed through the measurement of dielectric constant and dielectric strength and both show similar pattern of variation in different firing temperatures. Both dielectric constant and dielectric strength of mixes A, B, C and D increase at raising the firing temperature to 1200 $^o$C and drops down at firing temperature 1300 $^o$C (Figs. 15 and 16). The first increase in the electrical properties is attributed to the change in porosity of the test discs, because ceramic bodies with higher porosities have lower electrical properties (Novaković, R., *et al*., 1994) and their higher free silica content, as higher silica leads to higher relative permittivity, power factor-tan δ and dielectric strength (El-Arabaty, A., *et al*., 1975). Lower electrical properties at firing temperature 1300 $^o$C are most probably caused by the higher cordierite content in the test discs. Cordierite is known to have low electrical properties (Novaković, R., *et al*., 1994).

In mixes $C_1$, $C_2$, $D_1$ and $D_2$, were mineralizers are added, both dielectric constant and dielectric strength increase in comparison to mixes A, B, C and D. The increase in the dielectric constant is slight whereas dielectric strength almost doubles at lower firing temperature and becomes lesser at higher firing temperature. Dielectric constant and dielectric strength of the mixes with mineralizers decrease gradually at higher firing temperatures (Table 6), and this may be attributed to the increase of the cordierite phase in the test discs. The sharp decrease of the electrical properties in samples $C_2$ and $D_2$ at raising the firing temperatures is related to the amount of cordierite crystallized in the test discs too. The role of porosity is rather undetectable as the change of porosity is rather insignificant.

4958

*J. Appl. Sci. Res., 9(8): 4946-4959, 2013*
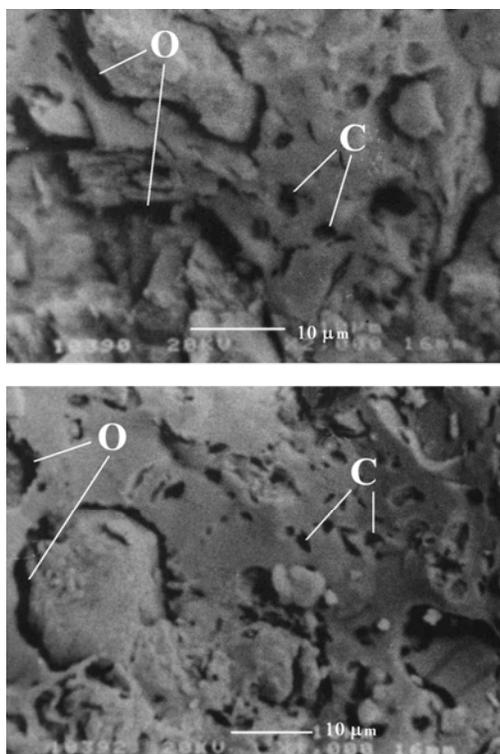
**Fig. 15:** Open (O) and closed (C) porosities in the cordierite samples.

**Table 6:** Dielectric constant and dielectric strength of the test discs fired at temperatures 1100°C, 1200°C and 1300°C.

| Mix | Firing temperature (°C) | | | | | |
|---|---|---|---|---|---|---|
| | 1100 | | 1200 | | 1300 | |
| | Dielectric constant | Dielectric strength KV/mm | Dielectric constant | Dielectric strength KV/mm | Dielectric constant | Dielectric strength KV/mm |
| A | 4.08 | 8.46 | 5.23 | 11.88 | 4.66 | 10.32 |
| B | 3.66 | 7.88 | 4.62 | 10.07 | 3.85 | 8.54 |
| C | 3.48 | 7.63 | 4.15 | 8.85 | 3.54 | 7.32 |
| D | 3.09 | 7.93 | 3.98 | 8.49 | 3.26 | 6.85 |
| $C_1$ | 5.21 | 15.78 | 4.83 | 14.23 | 4.52 | 12.57 |
| $C_2$ | 5.43 | 16.31 | 5.36 | 15.81 | 4.96 | 13.80 |
| $D_1$ | 4.94 | 13.98 | 4.72 | 12.63 | 4.36 | 11.71 |
| $D_2$ | 5.21 | 14.44 | 5.19 | 13.76 | 4.73 | 12.46 |

*Conclusions:*

Cordierite can be prepared from firing serpentinite, kaolinitic clay and bauxite, in proportions near to its stoichiometric composition, at 1300 °C. Addition of mineralizers, such as LiF (2 wt %) or LiF and NaF (1+1 wt %), facilitate the crystallization of cordierite at considerably lower firing temperature. Indialite becomes almost the only phase at 1300 °C. Thermal and electrical properties of the formed cordierite resemble those mentioned in the literature although the dielectric strength is higher than that quoted by Singer and Singer (1971) and Kingery *et al*. (1967) but within the range mentioned by Salmang (1961). Reduction of the porosity would improve the electrical properties of the test discs but would deteriorate their thermal properties.

Almost all mixes are suitable for refractory products, which needs low thermal expansion and high thermal shock resistance, and flameproof tableware but only mixes with the mineralizers can be utilized in electro-ceramics. Grinding the product, forming and reheating it can achieve further improvement.

**Refernces**

Aqrawi, A.M.A., 2001. Preparation and Study of Forsterite and Cordierite from Iraqi Serpentinites. Ph.D. thesis, Univ. of Baghdad, Iraq.

4959

*J. Appl. Sci. Res., 9(8): 4946-4959, 2013*

Barrier, J.C., J.L. Rehspringer, S. Vilminot and P. Poix, 1986. Synthesis and sintering comparison of cordierite powder. Material Research Society Symposium Proceedings, 73: 129-134.

Chester H.S., 1973. Refractories Production and Properties. Lund Humphries.

Dupon, R.W., R.L. McConville, D.J. Musolf, A.C. Tanous and M.S. Thompson, 1990. Preparation of cordierite below 1000 degree C via bismuth oxide flux.. Journal of the American Ceramic Society, 73(2): 335-339.

El-Arabaty, A., M. Baker, A. Nosser, S. El-Debeiky and I. Fouad, 1975. Effect of residual free silica on properties of porcelain insulators. Interceram, 4(2): 265-267.

Ferrari, A.M., L. Barbieri, C. Leonelli, T. Manfredini, C. Silrgardi and A.B. Corradi, 1997. Feasibility of using cordierite glass-ceramics as tile glaze. Journal American Ceramic Society, 80(7): 1757-1766.

Ghitulica, C., E. Andronescu, O. Nicola, A. Dicea and M. Birsan, 2007. Preparation and characterization of cordierite powders. Journal of the European Ceramic Society, 27(2-3): 711-713.

Grosjean, P., 1993. Cordierite ceramics. Interceram., 42(1): 11-15.

Khabas, T.A., V.I. Vereshchagin and O.V. Nevvonen, Synthesis of complex compounds in binary and ternary oxide systems doped with nanodisperse aluminum. Refractory and Industrial Ceramic, 45(2): 84-87.

Kingery, W.D., 1967. Introduction of Ceramics. John Wiley and Sons Inc

Kingery, W.D., H.K. Bowen and D.R. Uhlman, 1976. Introduction to Ceramics, John Wiley and Sons.

Kloss, W. S., 1974. Differential Thermal Analysis, Springer – Verlag.

Morell, R., 1979. The mineralogy and properties of sintered cordierite glass-ceramics. Proceedings of the British Ceramic Society, Mineralogy of Ceramics, No. 28: 53-71.

Naga, S.H., E.H. Sallam and D.M. Ibrahim, 1994. Effect of mineralizers on the production of dense cordierite bodies. Interceram, 43(4): 243-245.

Nakahara, M., Y. Kondo and K. Hamano, 1998. Effect of kaolin grain size on firing process and physical properties of cordierite ceramic. Journal of the Ceramic Society of Japan, 106(8): 787-791.

Nakahara, M., Y. Kondo and K. Hamano, 1999. Effect of particle size of powders ground by ball milling on densification of cordierite ceramic. Journal of the Ceramic Society of Japan, 107(4): 308-312.

Novaković, R., M. Atanasovska, M.V. Nikolic and M.M. Rishic, 1994. Influence of the cordierite phase on electric properties of the $MgO-Al_2O_3-SiO_2$ ceramic system. Interceram. 42(6): 464-465.

Salmang, H., 1961. Ceramics: Physical and Chemical Fundamentals. Butterworths.

Singer, F. and S. Singer, 1971. Industrial Ceramics. Chemical Publ. Co. Inc.

Trumbulović, Lj., Z. Aćimović, S. Panić and Lj Andrić, 2003. Synthesis and characterization of cordierite from kaolin and talc for casting application. Fac. Mechanicl Engineering Transactions, 31(1): 43-47.

Yamuna, A., R. Johnson, Y.R. Mahajan and M. Lalithambika, 2004. Kaolin-based cordierite for pollution control. Journal of the European Ceramic Society, 24(1):65-73.